

# RADIAL FORCE CONTROL OF BEARINGLESS MOTOR WITH FLUX EQUIVALENT AIR-GAP VIRTUAL WINDING CURRENT

**Huangqiu Zhu**

School of Electrical and Information Engineering, Jiangsu University, Zhenjiang 212013, China  
zhuhuangqiu@ujs.edu.cn

**Qiuliang Cheng, Qinghai Wu, Wei Pan**

School of Electrical and Information Engineering, Jiangsu University, Zhenjiang 212013, China  
wqh29902345@163.com

## ABSTRACT

A bearingless motor has two kinds of coupling windings, driving windings and bearing windings. The decoupling control for two sets of winding currents is difficult problem and key technology to stable operation of bearingless motors. A simple, reliable and accurate analyzing method for bearingless motors is put forward using the concept of flux equivalent air-gap virtual winding currents. Adopting this method, the operation condition  $P_B = P_M \pm 1$  for bearingless motor is quoted, and the necessary satisfied condition of generating a stable radial force in single direction on whole rotor's circumference is derived. On this basis, the control strategy of realizing bearingless motor's suspension operation is brought forward, and a prototype of bearingless surface-mounted permanent magnet synchronous motor is built and tested. The experiment results have shown that theory analysis of this strategy is accurate, a stable and reliable radial suspension force is obtained, and the validity and feasibility of this strategy is confirmed.

**KEY WORDS:** bearingless motor; permanent magnet-type synchronous motor; flux equivalent; winding current; radial suspension force; control

## INTRODUCTION

A bearingless motor has two kinds of coupling windings, driving windings and bearing windings. The coupling between these two kinds of winding currents is difficult problem to implement stable suspension operation of bearingless motors. Therefore, the decoupling control for two sets of winding currents is important research and key technology to stable suspension operation of bearingless motors. In literature [1], according to experiment measure, the relationship between radial force and quadratic difference of

magnetic flux density is linear for bearingless reluctance motor, which is similar to conventional magnetic bearings. On this basis, the function relation between magnetic flux density and magnetic potential is obtained by curve fitting of experiment measurement results. Thereout, when radial force is maximal, the function relation between force-stiffness and driving windings excitation current is deduced. Then, the conclusion is that the most effective radial force is gained when excitation current is 4~5A. This analysis method based on curve fitting and mathematics derivation has a definite theoretical guiding significance to estimate the control parameters of bearingless motor which structure has already decided. In literature [2], through the method of marking magnetic pole in circuit topological structure to research winding connection project of bridge configuration for single-phase bearingless motors. By marking driving winding flux linkage and bearing winding flux linkage in the motor structure scheme to research generating situation of radial forces. The basic characteristics of this bearingless motor can be validated by two-dimensional FEM analyzing method. Adopting these visual methods, analyzing bearingless motors becomes simple, direct, and can be understood more detail situation of air-gap flux. But control strategy research with this method is comparative difficulty<sup>3-6</sup>. In literature [7]: regarding permanent magnet flux linkage to equivalent current produced by driving windings, the function relation of radial forces is deduced by matrix equation of flux linkage. This method regarding flux linkage to equivalent winding current makes analyzing of bearingless motor visual and simple. But using it to mathematics derivation of flux linkage equation, the advantage of this method is not evident<sup>[2,8]</sup>. All the above proposed methods have complicated mathematics derivation and require experiment measurement to

confirm parameters. To research control strategy of bearingless motors, the proposed methods are not only miscellaneous in program, but also quite bad in flexibility.

For the sake of much more comprehensive research control strategy of bearingless motors and obtaining much more universal conclusions, an analysis method of bearingless motors based on concept of flux equivalent air-gap virtual winding currents is put forward in the paper. Adopting this method, further prove of various basic theories on bearingless motors will be given, and prevalent conclusions will be educed. To different type and different configuration of bearingless motors, intuitionistic, exact analysis will be given to produce situation of radial forces. Then, control strategy of effective radial suspension force is designed. This analysis method is based on distributing of air-gap flux, and is simple, exact and flexible. It has important guiding significance to FEM analysis of radial suspension force, experiment debugging and control optimize for bearingless motors.

The magnetic potential produced by full pitch windings distributes in rectangle wave, and main component is fundamental wave magnetic potential [9]. Considering each fundamental components of air-gap magnetic flux produced by each winding, the distribution of air-gap magnetic flux is produced by the currents in a series of air-gap virtual full pitch windings. That is, the distribution of air-gap magnetic flux is equal to the distribution of currents in a series of air-gap virtual full pitch windings, as shown in Fig.1. We suppose the virtual full pitch winding currents locating in the air-gap as flux equivalent air-gap virtual winding currents, treating it as DC, and the virtual full pitch windings can circumrotate, no mutual inductance among the virtual windings. Taking into account of fundamental wave magnetic potential which occupied main component, the error is small in practical situation, and it is convenient to synthesize the air-gap magnetic potential<sup>[10,11]</sup>. The foundation of flux equivalent air-gap virtual winding currents is that air-gap flux is uniformity and distribution symmetrical. The definitions about correlative concepts are listed in table 1.

**ANALYSIS METHOD WITH FLUX EQUIVALENT AIR-GAP VIRTUAL WINDING CURRENT**

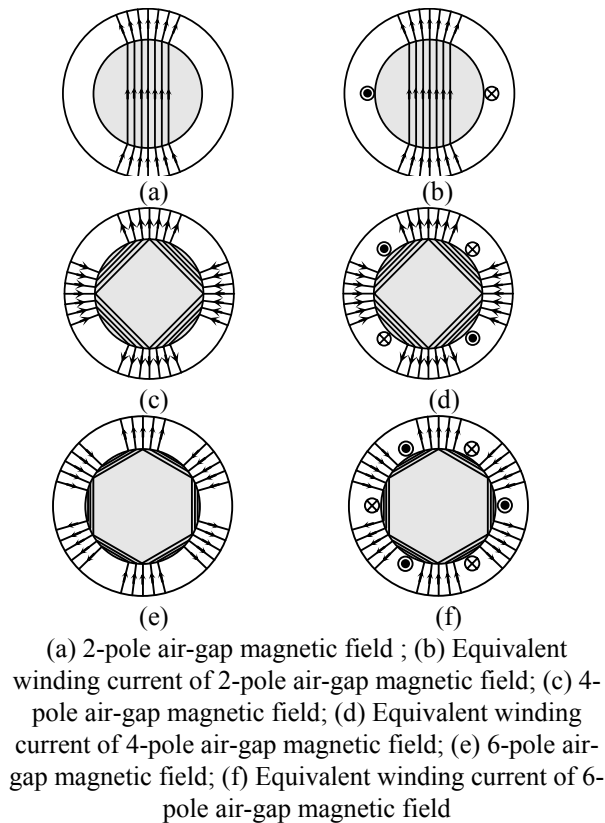
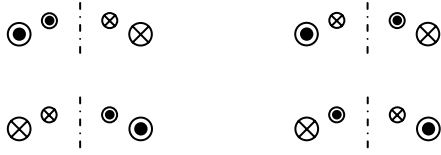


**FIGURE 1:** Schematic diagram of flux equivalent air-gap virtual winding current

**TABLE 1** Concepts about flux equivalent air-gap virtual winding currents

Concept	Definition
driving windings	produce torque in the stator
bearing windings	produce radial suspension forces
driving windings air-gap flux	air-gap flux that produced by current-carrying driving windings
bearing windings air-gap flux	air-gap flux that produced by current-carrying bearing windings
air-gap flux	composite flux of driving windings air-gap flux and bearing windings air-gap flux
equivalent virtual driving windings	virtual windings distributing in air-gap and as carrier of air-gap flux equivalent virtual winding current of driving windings
equivalent virtual bearing windings	virtual windings distributing in air-gap
A phase axes of driving windings	position that positive amplitude values of fundamental wave magnetic potential produced by driving winding currents when motor angle is $\omega t=0\text{rad}$
A phase axes of bearing windings	position that positive amplitude values of fundamental wave magnetic potential produced by bearing winding currents then motor angle is $\omega t=0\text{rad}$



(a) enhanced factors (b) weakened factors

**FIGURE 2:** Basic current structure formed by two sets of windings

Composite flux of equivalent virtual driving winding currents and equivalent virtual bearing winding currents may constitute basic structure form of all winding currents. When these two sets of windings form the structure of existing inclusion relation in space, it will appear maximal composite magnetic potential or minimum composite magnetic potential. If the center line of two sets windings is superposition, we named it enhanced factor or weakened factor (as shown in Fig.2, big dimension and small dimension of windings denote equivalent driving windings and equivalent bearing windings, respectively)<sup>[1,5,12]</sup>. If the center line of two sets windings is not superposition, we named it partial-enhanced factor or partial-weakened factor.

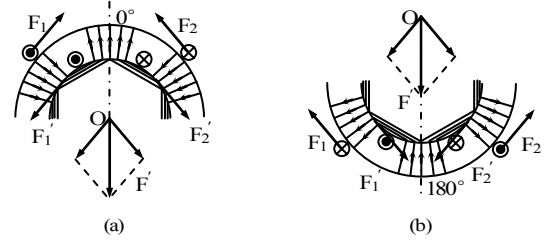
Supposing that the amplitude of fundamental wave magnetic potential produced by driving winding (pole-pair  $P_M$ ) current and bearing winding (pole-pair  $P_B$ ) current are  $F_M$  and  $F_B$ , respectively, and let positive amplitude values of two magnetic potential situate in air-gap position angle of  $\alpha=0$  rad. That is, form a structure of enhanced factor in air-gap position of  $\alpha=0$  rad. Then, the composite magnetic potential in air-gap is

$$f_M = F_M \cos(P_M \alpha) + F_B \cos(P_B \alpha) \quad (1)$$

Supposing  $F_M > F_B$  (If  $F_M < F_B$ , it is likely to appear situation of decreasing radial suspension forces as increasing bearing winding currents<sup>[11]</sup>), magnitude of  $F_B$  is considered as one unit, getting rid of  $(F_M - F_B) \cos(P_M \alpha)$ , then, the air-gap composite magnetic potential  $f_y$  can be described as follow

$$f_y = \cos(P_M \alpha) + \cos(P_B \alpha) \quad (2)$$

At the position of  $\alpha=0$ rad,  $f_y=2$ . Desiring to generating radial resultant force (Maxwell force, thereafter, all is Maxwell force if the character of the force is no explained) in single direction, due to the flux is uniformity and symmetrical, let  $f_y=0$  at position of  $\alpha=\pi$ rad. That is to say, it can and only can form an weakened factor at this position of  $\alpha=\pi$ rad. Namely, one of  $P_M$  and  $P_B$  is odd number, and the other is even number. That is, the discrepancy values of  $P_M$  and  $P_B$  must be an odd number. Nevertheless, when the difference value of  $P_M$  and  $P_B$  is more than 1, it will appear partial-enhanced factor and partial-weakening factor alternately at the exceptant positions of  $\alpha=0$ rad



(a) Lorentz force of enhanced factors; (b) Lorentz force of weakened factors

**FIGURE 3:** Schematic of the Lorentz force produced by equivalent virtual bearing windings when  $P_B < P_M$

and  $\alpha=\pi$ rad. Accordingly, it can't generate a stable radial force in single direction. Thus, the difference value of  $P_M$  and  $P_B$  must be 1. That is, it must satisfy the relation of  $P_B = P_M \pm 1$ . However, this relation has no restriction effect to homopolar-type bearingless motors and consequent-pole rotor bearingless motors<sup>[4,11]</sup>.

At position of  $\alpha=0$ rad, the basic current structure formed by two sets windings is enhanced factor. And at position of  $\alpha=\pi$ rad, the basic current structure formed by two sets windings is weakening factor. At this time, the direction of produced radial force is  $0^\circ$  (Through  $\alpha=\pi$  rad point to  $\alpha=0$  rad, all direction of radial force according to this definition). Based on left-hand rule and Newton's law, while  $P_B < P_M$ , Lorentz force which produced by equivalent bearing windings decreased the radial suspension force which formed by Maxwell force, shown in Fig.3 ( $F_1$  and  $F_2$  are Lorentz forces of equivalent bearing windings.  $F_1'$  and  $F_2'$  are their counterforce, respectively. And the action point locates in corresponding surface of rotor. The resultant force is  $F'$ ). And while  $P_B > P_M$ , Lorentz force which produced by equivalent bearing windings increased the radial suspension force which formed by Maxwell force. However, this conclusion is opposite to structure of external rotor motors<sup>[6]</sup>.

### RADIAL SUSPENSION FORCE CONTROL OF BEARINGLESS MOTOR WITH FLUX EQUIVALENT AIR-GAP VIRTUAL WINDING CURRENT

Supposing that the air-gap magnetic field produced by driving windings is stock-still and angular velocity is 0rad/s. Supposing that initial state is an enhanced factor at position of  $\alpha=0$ rad. Well then, there is a weakened factor at position of  $\alpha=\pi$ rad. At this time, the direction of produced radial force is  $0^\circ$ . If counter-clockwise is rotation positive direction. Then

(1) If  $P_B = P_M + 1$ , when equivalent virtual bearing windings rotate half polar distance in negative direction corresponding mechanical angle  $90^\circ/P_B$ , there is an enhanced factor at position of  $\alpha=-\pi/2$ rad (or two

axisymmetric partial-enhanced factors will appear both sides of position of  $\alpha=-\pi/2\text{rad}$ ). While there is a weakened factor at position of  $\alpha=\pi/2\text{rad}$  (or two axisymmetric partial- weakened factors will appear both sides of position of  $\alpha=\pi/2\text{ rad}$  ), i.e., the direction of radial force is  $-90^\circ$ . When equivalent virtual bearing windings rotate a polar distance in negative direction corresponding mechanical angle  $180^\circ/P_B$ , the enhanced factor at position of  $\alpha=0\text{rad}$  will become weakened factor. While the weakened factor at position of  $\alpha=-\pi\text{ rad}$  will become enhanced factor, i.e., the direction of radial force is  $-180^\circ$ . From this, we understand that when equivalent virtual bearing windings rotate in negative direction, rotational angular velocity of radial force is  $P_B$  times to that of equivalent virtual bearing windings, and the rotation direction is the same, vice versa.

(2) If  $P_B=P_M-1$ , when equivalent virtual bearing windings rotate half polar distance in positive direction corresponding mechanical angle  $90^\circ/P_B$ , there is an enhanced factor at position of  $\alpha=-\pi/2\text{rad}$  (or two axisymmetric partial-enhanced factors will appear both sides of position of  $\alpha=-\pi/2\text{rad}$ ). While there is a weakened factor at position of  $\alpha=\pi/2\text{rad}$  (or two axisymmetric partial- weakened factors will appear both sides of position of  $\alpha=\pi/2\text{ rad}$ ), i.e., the direction of radial force is  $-90^\circ$ . When equivalent virtual bearing windings rotate a polar distance in positive direction corresponding mechanical angle  $180^\circ/P_B$ , the enhanced factor at position of  $\alpha=0\text{rad}$  will become weakened factor. While the weakened factor at position of  $\alpha=-\pi\text{rad}$  will become enhanced factor, i.e., the direction of radial force is  $-180^\circ$ . From this, we understand that when equivalent virtual bearing windings rotate in positive direction, rotational angular velocity of radial force is  $P_B$  times to that of equivalent virtual bearing windings, and the rotation direction of radial force is opposite to that of the equivalent virtual bearing windings, vice versa.

Thereby, while the air-gap flux produced by driving windings is stock-still, rotational angular velocity of radial force is  $P_B$  times to that of equivalent virtual bearing windings (or air-gap flux produced by bearing windings). If  $P_B=P_M+1$ , the rotation directions of radial force and equivalent bearing windings are same. If  $P_B=P_M-1$ , the two directions of rotation are opposite, respectively.

Once more, supposing that air-gap flux produced by driving windings rotate in positive direction and angular velocity is  $\omega$ . If desiring to produce a stable radial force in single direction, namely keeping the steady direction, the absolute angular velocity of radial suspension force must be  $0\text{rad/s}$ . At this time, if taking air-gap flux produced by driving windings as reference object, the relative angular velocity of radial suspension force is -

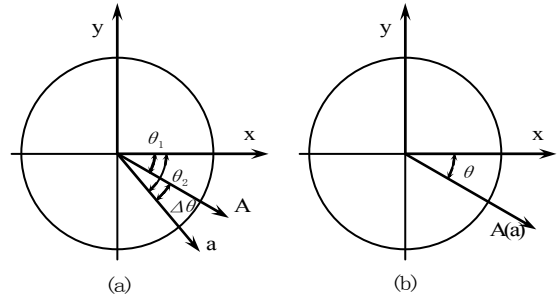


**FIGURE 4:** Relative position of driving windings and bearing windings

$\omega$ . That is to say, relative to that of bearing windings air-gap flux, radial suspension force rotates in negative direction of angular velocity  $\omega$ . Based on the proposed analysis, if  $P_B=P_M+1$ , relative to that of bearing windings air-gap flux, equivalent virtual bearing windings (or air-gap flux produced by driving windings) must be rotate in negative direction of angular velocity  $\omega/P_B$ . The absolute angular velocity is  $P_M\omega/P_B$ . If  $P_B=P_M-1$ , relative to that of bearing windings air-gap flux, equivalent virtual bearing windings (or air-gap flux produced by driving windings) must be rotate in positive direction of angular velocity  $\omega/P_B$ . The absolute angular velocity is  $P_M\omega/P_B$ .

From the proposed analysis, desiring to produce a stable radial force in single direction, the bearing windings air-gap flux will rotate in positive direction at the angular velocity of  $P_M\omega/P_B$ , and the electrical angular velocity is  $P_M\omega$ <sup>[13-15]</sup>. And that electrical angular velocity of the driving windings air-gap flux is  $P_M\omega$ . So, the necessary satisfied condition of generating a stable radial suspension force in single direction is that the bearing winding air-gap flux and driving windings air-gap flux have the same rotation directions, the rotating electric angular velocity is equal.

To synchronous motor, due to the rotational angular velocity of rotor is equal to that of the driving windings air-gap flux, The rotor rotational angular velocity can right be adopted for the control of bearing windings<sup>[13]</sup>. While to asynchronous motor, the stator rotating flux angular velocity can be adopted<sup>[9]</sup>.

To realizing radial suspension force control for bearingless motor unit,  $x$ - $y$  fixed coordinate on stator is set, shown in Fig.4. Supposing that angles between A phase axes of driving windings (named as A-axis) and a phase axes of bearing windings (named as a-axis) to  $x$ -axis are  $\theta_1$  and  $\theta_2$ , respectively. If  $\theta_1 \neq \theta_2$ , defined  $\Delta\theta = \theta_2 - \theta_1$ , shown in Fig.4 (a). Let currents in bearing windings compensate a mechanical angle  $\Delta\theta$ , accordingly, A-axis and a-axis are equal to superposition effective for air-gap magnetic field, shown in Fig.4(b). If  $P_B=P_M+1$ , let the increase of advance mechanical angle of bearing winding currents is  $\theta/P_B$  (or electrical angle is  $\theta$ ). If

$P_B=P_M-1$ , let the increase of lag mechanical angle of bearing winding currents is  $\theta/P_B$  (or electrical angle is  $\theta$ ). Then, the bearing windings air-gap flux and driving windings air-gap flux have the same rotating direction and the rotating electric angular velocity (namely, satisfied the necessary condition of generating a stable radial suspension force in single direction). The current component  $i_d$  of bearing windings will directly control the component of radial suspension force in  $x$ -axis. At the same time, due to current component  $i_q$  advance current component  $i_d$  with mechanical angle  $90^\circ/P_B$ , if  $P_B=P_M+1$ , current component  $i_q$  will produce a radial suspension force that advance  $x$ -axis  $90^\circ$  (that is direction of  $+y$ -axis). If  $P_B=P_M-1$ , current component  $i_q$  will produce a radial suspension force that lag  $x$ -axis  $90^\circ$  (that is direction of  $-y$ -axis).

To the bearingless motor operates at load, torque component  $i_q$  of driving winding currents will produce a flux linkage of  $q$ -axis. Thus, the driving windings air-gap flux generates an advance electrical angle of  $\theta$  less than  $90^\circ$ , which equal to lag mechanical angle  $\theta/P_M$  of equivalent virtual bearing windings relative to that of driving windings air-gap flux<sup>[14]</sup>. If  $P_B=P_M+1$ , the change angle value of radial suspension force is  $-\theta$ . To keep the direction of radial suspension force, we must add an advance time mechanical angle of  $\theta/P_B$  (or electrical angle  $\theta$ ) to bearing winding currents. If  $P_B=P_M-1$ , the change angle value of radial suspension force is  $\theta$ . To keep the direction of radial suspension force, we must add an advance mechanical angle of  $\theta/P_B$  (or electrical angle of  $\theta$ ) to bearing winding currents. From the proposed analysis, when the bearingless motor operates at load, in order to keep the direction of radial suspension force, the advance electrical angle of the bearing winding currents should equal to electrical angle of the driving windings air-gap flux. Because the bearingless motor operates at load, the advance electrical angle of the driving winding air-gap flux can be obtained by the proportion relation of flux linkage produced by torque component  $i_q$  and flux linkage produced by air-gap flux of original driving windings. Their proportion relation can be obtained by experimental measurement and calculate online. It's necessary to adopt corresponding nonlinear compensation control measure when there is flux saturation in existence.

## ANALYSIS OF EXPERIMENT RESULTS

A bearingless surface-mounted permanent magnet synchronous motor is built and the suspension operation is tested. Adopting two sets of current following inverters (CRPWM) to power driving windings and bearing windings, respectively, and DSP board as controller to realize the control strategy. The bearingless motor works at low speed and no load, torque

component  $i_q$  of driving windings is almost equal to zero, neglecting advance electrical angle of air-gap flux produced by driving windings. Then, nearly all the air-gap flux produced by driving windings is powered by permanent magnet of the rotor. The rotation state of the air-gap flux produced by driving windings is obtained through measuring rotor position<sup>[2]</sup>.

The bearingless permanent magnet synchronous motor in this experiment is three-phase AC motor. And pole-pair numbers of driving windings and bearing windings are 2 and 3, respectively. A-axis of driving windings and a-axis of bearing windings are superposition and the lag angle to  $x$ -axis is  $35^\circ$ . If rotor rotates in positive direction and the angular velocity is  $\omega$ , then, the rotational angular velocity of air-gap flux produced by driving windings is also  $\omega$ . Based on the necessary satisfied condition of generating a stable radial suspension force in single direction, let the electrical angle velocity of the air-gap flux produced by bearing windings rotates in positive direction at the speed of  $2\omega$ , then, the rotor can be suspended by closed loop control.

To validate the correctness of this analysis method, the electrical angle velocity of the air-gap flux produced by bearing windings rotates in negative direction at the speed of  $2\omega$ , and the magnitude of radial force is constant. Under this circumstance, the angular velocity of equivalent virtual bearing windings to equivalent virtual driving windings is  $-5\omega/3$ , and absolute angular velocity of the produced radial force is  $-4\omega$ . The given normalized value of bearing winding currents component of  $d$ -axis  $i_d$  is 0.7, component of  $q$ -axis  $i_q$  is 0. The DC generatrix voltage will be changed from 0V to 20V in the inverter which powers the bearing windings. Then, the waveform of rotor displacement in  $x$ -direction is shown in Fig.5.

From Fig.5, when bearing windings are electrified, the waveform of rotor displacement appears a component of four times to angular velocity of the rotor, which is effect of radial suspension force. It inosculates

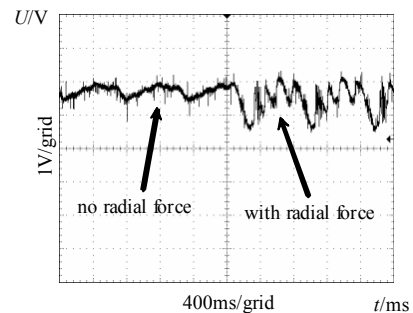
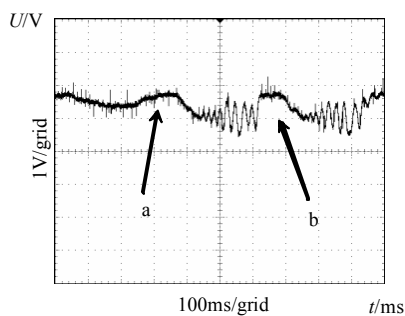


**FIGURE 5:** Waveform of rotor displacement in the  $x$ -direction as air-gap flux produced by bearing windings rotates in reverse direction

to proposed analysis. So the correctness of the proposed analysis method is validated. Thereinto, the emergence of periodic change at the time of no radial force is brought by mechanical imbalance of the motor. And change period is decided by rotate speed of rotor<sup>[15]</sup>. Besides, whole of this waveform offsets upward (maximal offset of rotor corresponding to 0.6V and 2.1V in this waveform). Only when radial force is added, the rotor will appear maximal offset. Also, in rotating period of four radial forces within a circle rotating of rotor, there is only a wave trough and a wave crest reach the maximal offset, other three wave troughs and three wave crests are offset upward. It accounts for that there is a biggish force in a certain fixed radial direction of motor.

To realizing the suspension of rotor, we adopt closed loop control to rotor displacement. By defining offset of rotor displacement in  $x$ -direction relative to center of stator is  $x$ , then, the maximal offset of rotor displacement through eddy current sensor and interface circuit to controller, the received absolute value of digital quantity is 204. For the easy understand of the control strategy, we adopt simple fuzzy control rule: when  $x < -32$ , the output is 0.7 ( $i_d$ , the given normalized value of bearing winding currents component of  $d$ -axis, the same below); when  $-32 < x < -24$ , the output is 0.587; when  $-24 < x < -16$ , the output is 0.46; when  $-16 < x < -8$ , the output is 0.3; when  $-8 < x < 8$ , the output is 0; when  $8 < x < 16$ , the output is -0.3; when  $16 < x < 24$ , the output is -0.46; when  $24 < x < 32$ , the output is -0.587; when  $x > 32$ , the output is -0.7. The DC generatrix voltage will be changed from 0V to 20V in the inverter which powers the bearing windings. Then, the waveform of rotor displacement in  $x$ -direction is shown in Fig.6.

In Fig.6, we know that the produced radial suspension force is able to restrict the rotor alternating motion near the centre position and its motive amplitude has a definite range. If a differential control block is added, motive amplitude will be reduced more; finally, the stable suspend operation is realized. This experiment



(a) no radial suspension force; (b) with radial suspension force

**FIGURE 6:** Waveform of rotor displacement in  $x$ -direction with closed loop control

testified the correctness and feasibility of the radial suspension force control strategy to bearingless motors. However, due to the existence of imbalance and other factors in motor, it caused the rotor nears to stator verge in a certain fixed position at the condition of no optimal design to experiment motor. It accounts for that the proposed biggish force in above experiment has an influence on suspension effect of motor rotor<sup>[1]</sup>. Further more, when offset in center of the rotor exceed a certain value, it is likely to appear a negative stiffness in radial force and make suspension performance worse. But this has no influence to the correctness of proposed radial suspension force control strategy to bearingless motors.

## CONCLUSIONS

Based on the analysis method with flux equivalent air-gap virtual winding current, and the operation condition  $P_B = P_M \pm 1$  for bearingless motor is quoted, the influence of Lorentz force produced by bearing windings on radial suspension force is analysed. The necessary condition of concerning the electrical angular velocity of the air-gap flux produced by bearing windings and generating a stable radial suspension force with single direction is deduced. On this basis, to the distribution of two sets windings, the increase of advance or lag angle to bearing winding currents for realizing the control of the radial suspension force is given. Through analyzing the impact of the flux linkage generating by torque current component of the driving windings on load operation over the air-gap flux produced by driving windings, in order to keep the direction of radial suspension force, the advance electrical angular of bearing windings must equal to that of the air-gap flux produced by driving windings. A bearingless surface-mounted permanent magnet (SPM) synchronous motor is designed. Through the revolving experiment of radial suspension force, the correctness of the proposed analysis method in this paper is verified. Moreover, through the closed loop control experiment of rotor displacement, the feasibility and the correctness of radial suspension force control strategy of bearingless motor are verified. This analysis method has many advantages, such as simple, accurate, flexible, and can accurate analysis and reliable control to radial suspension force of different types and configurations bearingless motors. It has important guiding significance to FEM analysis, experiment test, control optimization for the bearingless surface-mounted permanent magnet (SPM) synchronous motor. This control strategy lays a foundation for reliable and stable suspend operation for bearingless motors.

## ACKNOWLEDGEMENTS

This research is sponsored by the NSFC (Grant No. 50575099) and the National High Technology Research

and Development of China (863 Program) (Grant No. 2007AA04Z213).

## REFERENCES

1. Chiba A., Hanazawa M., Fukao T. and Rahman M. A., Effects of Magnetic Saturation on Radial Force of Bearingless Synchronous Reluctance Motors, *IEEE Transactions on Industry Applications*, 1996,32(2):354-362
2. Khoo W. K. S., Bridge Configured Winding for Polyphase Self-bearing Machines, *IEEE Transactions on Magnetics*,2005,41(4):1289-1295
3. Ferreira J. M. S., Zucca M., Salazar A. O. and Donadio L., Analysis of a Bearingless Machine with Divided Windings, *IEEE Transactions on Magnetics*,2005,41(10):3931-3933
4. Asami K., Chiba A., Rahman M. A., Hoshino T. and Nakajima A., Stiffness Analysis of a Magnetically Suspended Bearingless Motor with Permanent Magnet Passive Positioning, *IEEE Transactions on Magnetics*,2005,41(10):3820-3822
5. Takemoto M., Chiba A., Akagi H. and Fukao T., Radial Force and Torque of a Bearingless Switched Reluctance Motor Operating in a Region of Magnetic Saturation, *IEEE Transactions on Industry Applications*,2004,40(1):103-112
6. Ooshima M., Kitazawa S., Chiba A., Fukao T. and Dorrell D. G., Design and Analyses of a Coreless-stator-type Bearingless Motor/Generator for Clean Energy generation and storage systems, *IEEE Transactions on Magnetics*,2006,42(10):3461-3463
7. Oshima M., Miyazawa S., Deido T., Chiba A., Nakamura F. and Fukao T., Characteristics of a Permanent Magnet Type Bearingless Motor, *IEEE Transactions on Industry Applications*,1996,32(2):363-370
8. Ooshima M., Chiba A., Fukao T. and Rahman A., Design and Analysis of Permanent Magnet-Type Bearingless Motors, *IEEE Transactions on Industrial Electronics*,1996,43(2):292-299
9. Fahai Li and Yan Wang. Basic of Motor and Drag (Secondly edition),Beijing: Qinghua Publishing Company,2003 (in Chinese)
10. Chiba A., Kiryu K., Rahman M. A. and Fukao T., Radial Force and Speed Detection for Improved Magnetic Suspension in Bearingless Motors, *IEEE Transactions on Industry Applications*,2006, 42(2):415-422
11. Ichikawa O., Chiba A. and Fukao T., Inherently Decoupled Magnetic Suspension in Homopolar-Type Bearingless Motors, *IEEE Transactions on Industry Applications*,2001,37(6):1668-1674
12. Inagaki K., Chiba A., Rahman M. A. and Fukao T., Performance Characteristics of Inset-Type Permanent Magnet Bearingless Motor Drives, *IEEE Power Engineering Society Winter Meeting*, Singapore, 2000,1:202-207
13. Ooshima M., Chiba A., Rahman A. and Fukao T., An Improved Control Method of Buried-Type IPM Bearingless Motors Considering Magnetic Saturation and Magnetic Pull Variation, *IEEE Transactions on Energy Conversion*,2004,19(3):569-575
14. Suzuki T., Chiba A., Rahman M. A. and Fukao T., An Air-Gap-Flux-Oriented Vector Controller for Stable Operation of Bearingless Induction Motors, *IEEE Transactions on Industry Applications*,2000,36(4):1069-1076
15. Chiba A., Furuichi R., Aikawa Y., Shimada K., Takamoto Y. and Fukao T., Stable Operation of Induction-Type Bearingless Motors Under Loaded Conditions, *IEEE Transactions on Industry Applications*,1997,33(4):919-924